



Experimental Study of Detecting Rainfall Using Microwave Links: Classification of Wet and Dry Periods

Kun Song , Xichuan Liu , Mingzhong Zou, Ding Zhou, Haonan Wu, and Feng Ji

Abstract—To improve the accuracy of rainfall estimation by microwave links, this article presents a method for classifying wet and dry periods based on the support vector machine (SVM). The average, minimum, and maximum attenuation measurements in 5 min are applied as the feature vector of the SVM after the analysis of the relation between the statistical parameters of the attenuation measurements from seven microwave links and the wet/dry periods. When the baseline attenuation is needed for retrieving the path-averaged rain rate, the method can classify the wet/dry periods and estimate a dynamic baseline with an optimal combination of the statistical parameters of the attenuation measurements based on the prior training. Experiments are conducted to test the classification method. The results show that the classification accuracy is higher than 0.8, which is a satisfactory result. Most values of the true positive rate are higher than 0.9, which indicates that the method can correctly classify most of the wet periods. Additionally, the values of the false positive rate are less than 0.3, and most of the values are less than 0.2, suggesting that the method incorrectly classifies the dry period as the wet period with a low probability. The results demonstrate that the classification method is capable of classifying the wet and dry periods with a high accuracy, which can help improve the precision of the baseline of microwave links and rainfall estimation.

Index Terms—Classification of wet and dry period, microwave link, rain detection, support vector machine (SVM).

I. INTRODUCTION

RAINFALL monitoring is important for meteorology, hydrology, and climate research. Several methods have been developed for estimating the rainfall. Rain gauges are considered to provide accurate ground point measurements. However, they do not provide high spatial resolution data and the number of rain gauges is declining in many areas [1], [2]. The weather

radar provides high temporal and spatial rainfall data but is affected by the ground clutter and does not provide accurate ground-level measurements [3], [4]. Meteorological satellites offer an increase in the rainfall coverage and spatial-temporal resolution of rainfall data and provide rainfall estimation over vast oceanic areas, where radar networks are not available [2]. However, measurement errors and sampling uncertainties limit the application of satellites [5]. Therefore, alternative, complementary, and ground-based ways for monitoring rainfall are necessary.

Since 2006, rainfall estimation by microwave links (MLs), from 10 to 30 GHz, has been investigated due to the ever-increased availability of power measurements that are stored and delivered by cellular communication operators for research purposes [6]–[9]. This application can not only estimate the path-average rainfall intensity but also reconstruct rainfall maps [10]–[15]. Moreover, MLs have been applied for correcting the attenuation of weather radar reflectivity and detecting faulty rain gauges; and earth-space links have been involved in monitoring the rainfall [16], [17]. The applications of MLs for observing the rainfall have the following advantages: redundancy, complementarity, timeliness, and cost of information [18].

In reality, MLs, which belong to telecommunication operations, are uncertain because their original purpose is optimized for the performance of communication rather than monitoring the rainfall. Thus, many researchers study the uncertainties of MLs, such as baseline variations [19]. A baseline is the average attenuation of the ML in nonrainy periods and lowering the uncertainty of the baseline attenuation is necessary to improve the estimation accuracy. Thus, the key to obtaining an accurate baseline is the classification of wet (rainy) and dry (nonrainy) periods. Cherkassky *et al.* [18] summarize that the classification methods include spectral analysis [20], statistical analysis [1], [21], multifamily likelihood ratio tests [22], and additional side information provided by the weather radar or rain gauges [23].

In this article, we adopt the support vector machine (SVM) for classifying the wet and dry periods using MLs, which is a machine learning way and allocates complex analysis processes to computers. SVM is a supervised learning model with learning algorithms that can analyze data for classification, particularly for small samples [24], [25]. First, we analyze the relation between the statistical parameters of the attenuation data from seven MLs and the wet/dry periods and select statistical

Manuscript received March 29, 2020; revised June 5, 2020 and August 20, 2020; accepted August 28, 2020. Date of publication September 3, 2020; date of current version September 17, 2020. This work was supported by National Natural Science Foundation of China under Grant 41975030, Grant 41505135, and Grant 41475020 and in part by National Natural Science Foundation of Jiangsu Province under Grant BK20181337. (Corresponding author: Xichuan Liu.)

Kun Song and Xichuan Liu are with the College of Meteorology and Oceanography, National University of Defense Technology, Nanjing 210000, China (e-mail: songkun_0521@foxmail.com; liuxc2012@hotmail.com).

Mingzhong Zou is with the River Management Division, Jiangyin 214400, China (e-mail: 275484685@qq.com).

Ding Zhou, Haonan Wu, and Feng Ji are with the Weizhirun Intelligent Technology Company, Ltd., Jiangyin 214434, China (e-mail: 282202922@qq.com; 2252626203@qq.com; 2436428357@qq.com).

Digital Object Identifier 10.1109/JSTARS.2020.3021555

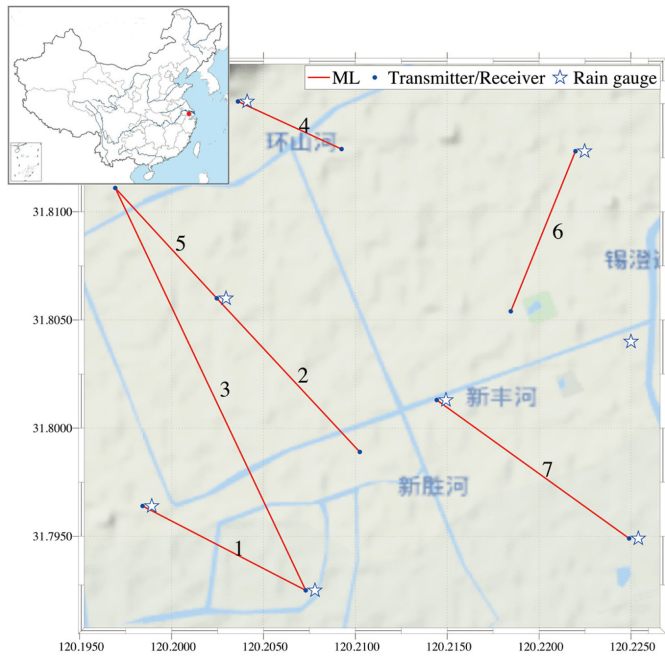


Fig. 1. Details of the seven MLs and eight rain gauges. The red line represents the ML and the blue asterisk represents the transmitter or receiver of the ML. The pentagram represents the rain gauge. The red point of the figure in the upper left corner shows the location of Jiangyin, China.

parameters, such as the mean values of the attenuation measurements, as the feature vector. Second, the SVM is employed to classify wet/dry periods by the feature vector. Finally, experiments are conducted to test the proposed method.

The rest of this article is organized as follows. Section II introduces the data of attenuation measured by MLs and details of the classification method for wet and dry periods. Section III tests the method. Section IV compares the classification results by different kinds of statistical parameters and discusses the influence of the frequency and length of MLs. A comparison with other classification methods is conducted. Section V concludes the article.

II. MATERIAL AND METHODS

A. Data

A total of 15 horizontal polarization MLs, which range from 15 to 23 GHz, are applied for classifying wet/dry periods in Jiangyin, China, from March to April 2019 and July to September 2019. The base towers are operated by China Mobile. The resolution of the transmitter and receiver is 0.1 dBm and the sampling frequency is approximately one time per minute. In the experimental area of the study, there are many trees and buildings, which can cause the multipath propagation of microwave signals and increase the attenuation, even in dry periods. Thus, seven line-of-sight MLs are selected for testing the classification method. The locations of seven MLs are given in Fig. 1, and the lengths and frequencies of the MLs are given in Table I. The attenuation measurements of MLs can be obtained by subtracting the receiving power from the transmitting power. Eight rain

TABLE I
SEVEN LINKS FOR CLASSIFICATION

ML	1	2	3	4	5	6	7
frequency (GHz)	15	15	18	23	23	23	23
length (km)	0.94	1.08	2.29	0.59	0.77	0.89	1.22

gauges are installed near the MLs to verify the accuracy of the classification of the wet and dry periods. The resolution of the gauge is 0.5 mm and the time accuracy is 1 time per 5 min. The locations of the rain gauges are shown in Fig. 1. The wet period is defined when five or more rain gauges measure more than 0 mm in 5 min. In the study, 14 days in 2019 (March 27, April 9, 21, and 22, July 17–19, August 25, 27, and 28, and September 1, 2, 4, and 5) are selected to test the classification method because there are more than 2 h of rainfall in a given day. Both of the attenuation measurements by the MLs and the rainfall estimation by the rain gauges in the study are based on these days.

B. Statistical Analysis Between the Attenuation Measurements and the Wet/Dry Periods

The attenuation measured by MLs is composed of rain-induced attenuation and attenuation other than rain, such as water vapor content, air temperature, and wet antenna attenuation [26]–[28]. The microwave signal is attenuated additionally by the absorption and scattering of raindrops in its transmission path on rainy periods. The rain-induced attenuation ratio of the ML can be calculated by (1) [29]:

$$A = a \cdot R^b \quad (1)$$

where A (dB/km) is the rain-induced attenuation ratio of the transmission path, R (mm/h) is the path-average rainfall intensity, and a and b are the coefficients related to the frequency of the ML and the raindrop size distribution, respectively. Since rainfall attenuates the signal of the ML, the values of the attenuation vary in different weather conditions (rainy and nonrainy), which can be applied to classify wet and dry periods. For further analysis of the relation between the attenuation of MLs and the wet/dry periods, the mean value, standard deviation, minimum value, and maximum value from 5-min attenuation are calculated [30], [31]. Fig. 2 shows the histograms of these four parameters in wet or dry periods of the seven MLs and a normal fitting is adopted for two conditions. The mean values of seven MLs in wet periods are higher than those in dry periods, which is consistent with the finding that the attenuation measurements in rainy periods are larger than those in dry periods. The small overlap of the two histograms indicates a strong correlation between the mean values and the wet/dry periods. In addition, the fitted curves show that the mean values of the normal distribution in wet periods are also higher than those in dry periods, which manifests that the mean value of 5 min can be adopted to classify wet and dry periods. Fig. 2 also shows that the characteristics of the minimum and maximum values are similar to that of the mean values, which means that these two parameters correlate with the wet

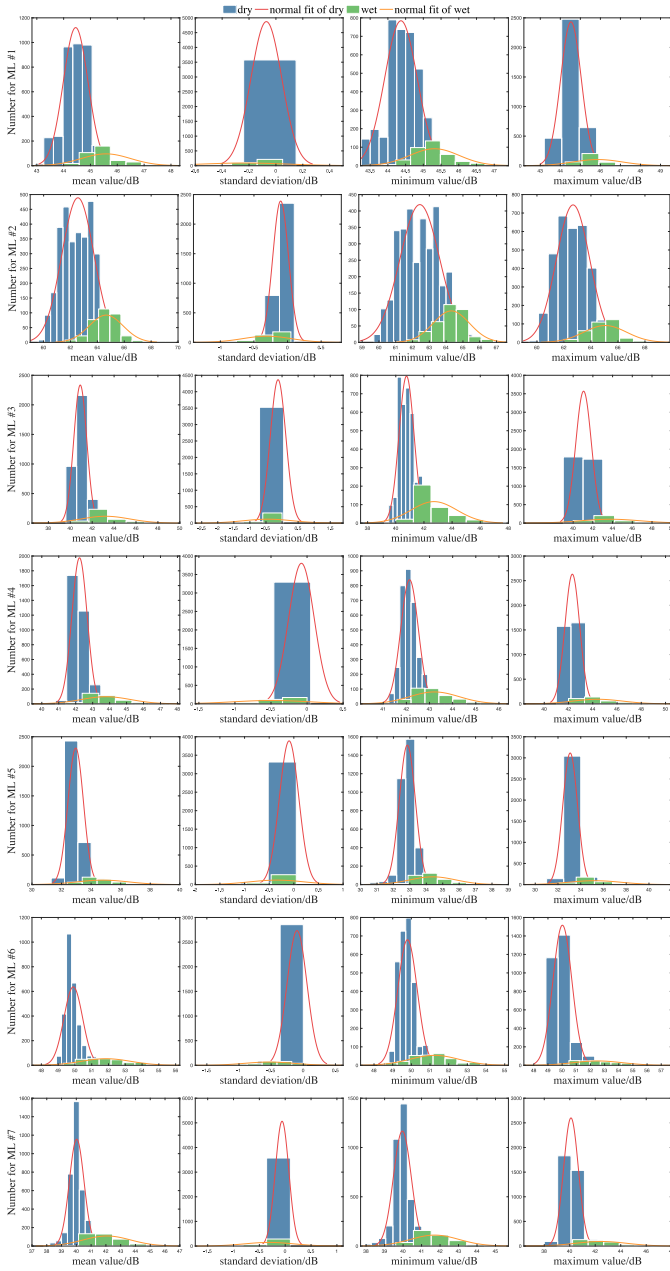


Fig. 2. Histograms of statistical parameters of the seven MLs (wet/dry period).

and dry periods, and can be applied for classifying the wet/dry periods. However, a large part of the histograms of the standard deviation overlaps, which implies that the standard deviation is not suitable for the classification in this study.

C. Classification Method of Wet and Dry Periods Based on SVM

As indicated by the aforementioned analysis, the mean, minimum, and maximum values of the seven MLs relate to the wet and dry periods, which are suitable for the classification. Therefore, we can set a single parameter (one of the three statistical parameters in the classification) or multiple parameters (the combination of the mean, minimum, and maximum

values) as feature vectors for the classification. In the study, the SVM is adopted for classifying wet and dry periods because the feature vector of SVM can be one or more parameters. The SVM is an extensively employed machine learning method with a set of linear indicator functions for the classification and regression analysis [32]. The SVM maps the input data into a high-dimensional feature space where a hyperplane is constructed. The optimal linear hyperplane is employed to separate the original input space and the kernel function is applied to transform data into different classes [33]. The accuracy of the SVM is dependent on suitable kernel functions, which include polynomial kernel, sigmoid kernel, radial basis function, and linear kernel. In this study, a radial basis function is adopted for transforming data. Compared with other machine learning methods, the SVM is more suitable for the data with a small sample, for example, the wet/dry classification in the study.

We set $\mathbf{x}_{T,i}$ and $y_{T,i}$ as the training set, where $\mathbf{x}_{T,i}$ are the feature vectors that consist of statistical parameters, $y_{T,i}$ are the labels of wet and dry periods, and i represents the time series. The training set is applied to construct a classification function for wet/dry periods. First, we construct and solve the optimal solution of the convex quadratic programming problem

$$\begin{aligned} \min_{\alpha} \quad & \frac{1}{2} \sum_{i=1}^N \sum_{j=1}^N \alpha_i \cdot \alpha_j \cdot y_{T,i} \cdot y_{T,j} \cdot K(\mathbf{x}_{T,i}, \mathbf{x}_{T,j}) - \sum_{i=1}^N \alpha_i \\ \text{s.t.} \quad & \begin{cases} \sum_{i=1}^N \alpha_i \cdot y_{T,i} = 0 \\ 0 \leq \alpha_i \leq C, i = 1, 2, \dots, N \end{cases} \end{aligned} \quad (2)$$

where $K(\cdot)$ is the kernel function and C is a penalty parameter, which is greater than zero. In this study, a Gaussian kernel function is adopted. Thus, the optimal solution α^* is solved by (2). The weight of the classification function can be calculated as follows:

$$\mathbf{w}^* = \sum_{i=1}^N \alpha_i^* \cdot y_{T,i} \cdot \mathbf{x}_{T,i}. \quad (3)$$

Second, the constant threshold b can be calculated as

$$b^* = y_{T,j} - \sum_{i=1}^N \alpha_i^* \cdot y_{T,i} \cdot K(\mathbf{x}_{T,i}, \mathbf{x}_{T,j}). \quad (4)$$

Finally, the classification function is obtained as

$$f(\mathbf{x}) = \text{sgn} \left(\sum_{i=1}^N \alpha_i^* \cdot y_{T,i} \cdot K(\mathbf{x}_{T,i}, \mathbf{x}) + b^* \right) \quad (5)$$

when $f(\mathbf{x}) = 1$ or -1 , the classification result represents a wet period or a dry period, respectively.

III. RESULTS

The classification method is applied to classify wet and dry periods by using the MLs mentioned in Table I. In the study, we set half of the data as the training set and set the remaining half as the testing set. Moreover, the study exploits the classification accuracy of the single-parameter and multiple-parameter classification methods.

Classification results by mean		Classification results by minimum		Classification results by maximum		
	Negative (dry)	Positive (wet)	Negative (dry)	Positive (wet)	Negative (dry)	Positive (wet)
Actual: (dry)	857 86.6%	133 13.4%	819 82.7%	171 17.3%	880 88.9%	110 11.1%
Actual: (wet)	9 6.1%	139 93.9%	7 4.7%	141 95.3%	12 8.1%	136 91.9%
	(a)	(b)	(c)			

Fig. 3. Confusion matrixes of the classification results by three parameters of the ML #3. (a) Classification results by mean. (b) Classification results by minimum. (c) Classification results by maximum. TP: the number of wet periods is correctly classified as the wet period; FP: the number of dry periods is incorrectly classified as the wet period; TN: the number of dry periods is correctly classified as the dry period; FN: the number of wet periods is incorrectly classified as the dry period. The percentage below the number of the classification in each grid represents the fraction of relevant instances that have been classified over the total number of relevant instances [e.g., (wet period correctly classified as the wet period)/(all wet period)].

A. Classification Results by Single-Parameter Method

We set the mean, minimum, and maximum values as the feature vector to classify the wet and dry periods by seven MLs based on the SVM. We know that the confusion matrix, which consists of the true positive (TP), false positive (FP), true negative (TN), and false negative (FN), allows the visualization of the performance of the supervised classification model and can avoid a misleading result if the classification has an unequal number of observations in each class. The confusion matrixes of the classification results by three parameters of ML #3 are shown in Fig. 3. The results indicate that the single-parameter method can classify correctly most of the wet and dry periods by ML #3. Moreover, there is no significant difference in the classification results among the mean, minimum, and maximum values.

For further analysis of the results of all seven links, we calculate the accuracy, TP rate (TPR), and FP rate (FPR) of the classification results. The calculation of these evaluation parameters is given as follows [34]:

$$\begin{aligned} \text{accuracy} &= \frac{TP + TN}{TP + FP + TN + FN} \\ \text{TPR} &= \frac{TP}{TP + FN} \\ \text{FPR} &= \frac{FP}{TN + FP}. \end{aligned} \quad (6)$$

Accuracy is the ratio of the correct classifications to the total number of wet and dry periods. The TPR, which is also referred to as sensitivity or recall, is applied to measure the percentage of the actual wet periods, which are correctly classified. The FPR is employed to measure the percentage of the actual dry periods, which are incorrectly classified. These three evaluation parameters can evaluate the overall performance of the classification method. Fig. 4 and Table II illustrate the evaluation parameter of seven links by the mean, minimum, and maximum values. Most of the values of accuracy are higher than 0.8, which indicates a high classification accuracy. The values of

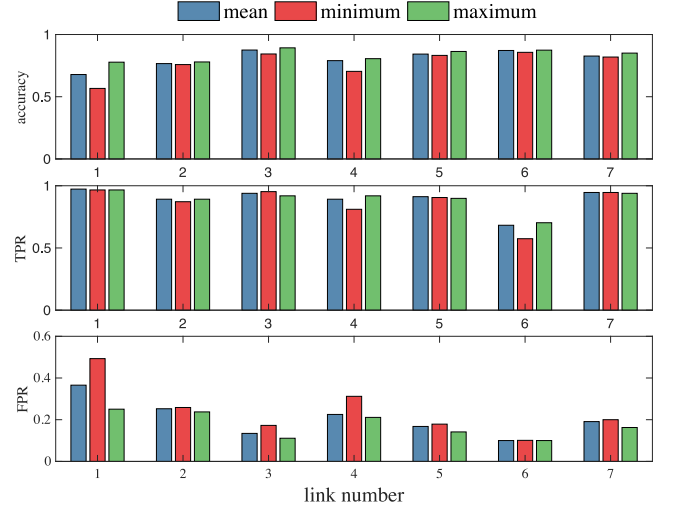


Fig. 4. Accuracy, TPR, and FPR of seven links by the mean, minimum and maximum value, respectively.

TABLE II
CLASSIFICATION RESULTS BY SINGLE-PARAMETER METHOD

	ML	1	2	3	4	5	6	7
Accuracy	mean	0.68	0.77	0.88	0.79	0.84	0.87	0.83
	min	0.57	0.76	0.84	0.70	0.83	0.86	0.82
	max	0.78	0.78	0.89	0.81	0.86	0.87	0.85
TPR	mean	0.97	0.89	0.94	0.89	0.91	0.68	0.95
	min	0.97	0.87	0.95	0.81	0.91	0.57	0.95
	max	0.97	0.89	0.92	0.92	0.90	0.70	0.94
FPR	mean	0.37	0.25	0.13	0.23	0.17	0.10	0.19
	min	0.49	0.26	0.17	0.31	0.18	0.10	0.20
	max	0.25	0.24	0.11	0.21	0.14	0.10	0.16

TPR are near to 0.9 in most results, which implies that most of the wet periods are correctly classified. Additionally, a large number of FPRs are less than 0.2, which means a low probability of dry periods is classified incorrectly similar to wet periods. The results reveal that although the classification results by three parameters exhibit no significant difference, the maximum value is the optimal option according to the overall effect. It is similar to the conclusion of a recent study, which suggests that the maximum attenuation at higher frequencies provides more information about the rainfall than the minimum attenuation [35]. Moreover, this conclusion has been proven theoretically [36].

B. Classification Results by Multiple-Parameter Method

In addition to the single-parameter method, the multiple-parameter method is also adopted in the study. Table III gives four combinations of the mean value, the minimum value, and the maximum value employed in the classification method. The confusion matrixes of the classification results by four combinations of ML #3 are shown in Fig. 5. Similar to Fig. 3, four combinations of ML #3 can correctly classify most of the wet and dry periods, and four classification results have no significant difference.

TABLE III
COMBINATIONS OF THE MEAN, MINIMUM, AND MAXIMUM VALUES

	Combination 1	Combination 2	Combination 3	Combination 4
mean	√	√		√
min	√		√	√
max		√	√	√

Mean, min, and max in the table represent the mean value, minimum value, and maximum value, respectively.

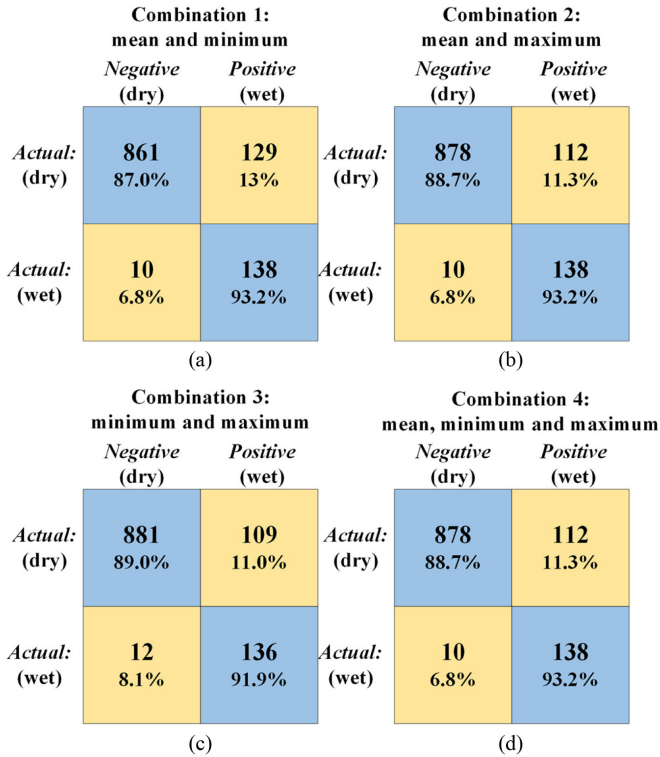


Fig. 5. Confusion matrixes of the classification results by four combinations of the mean, minimum, and maximum values of ML #3.

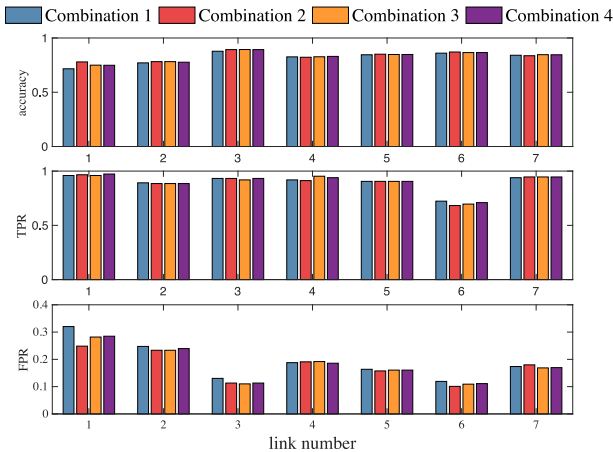


Fig. 6. Accuracy, TPR, and FPR of seven links by four combinations.

TABLE IV
CLASSIFICATION RESULTS BY MULTIPLE-PARAMETER METHOD

	ML	1	2	3	4	5	6	7
Accuracy	c-1	0.72	0.77	0.88	0.83	0.85	0.86	0.84
	c-2	0.78	0.78	0.89	0.82	0.85	0.87	0.84
	c-3	0.75	0.78	0.89	0.83	0.85	0.87	0.85
	c-4	0.75	0.78	0.89	0.83	0.85	0.87	0.85
TPR	c-1	0.96	0.89	0.93	0.92	0.91	0.72	0.94
	c-2	0.97	0.89	0.93	0.91	0.91	0.68	0.95
	c-3	0.96	0.89	0.92	0.95	0.91	0.70	0.95
	c-4	0.97	0.89	0.93	0.94	0.91	0.71	0.95
FPR	c-1	0.32	0.25	0.13	0.19	0.16	0.12	0.17
	c-2	0.25	0.23	0.11	0.19	0.16	0.10	0.18
	c-3	0.28	0.23	0.11	0.19	0.16	0.11	0.17
	c-4	0.28	0.24	0.11	0.19	0.16	0.11	0.17

c-1, c-2, c-3, and c-4 represent combinations 1, 2, 3, and 4, respectively.

Fig. 6 and Table IV give the accuracy, TPR, and FPR of the seven links by four combinations. All values of accuracy are higher than 0.7 and most of the values are greater than 0.8, which imply that the combinations of the three parameters classify wet and dry periods with high accuracy. All TPRs are near to 0.7 and most values are higher than 0.9, which indicate that most wet periods are correctly identified by the combinations. Moreover, almost all FPRs are less than 0.3 and the minimum value of FPR is 0.1, which elaborate that a small number of dry periods are classified incorrectly as wet periods. In addition, as shown in the figure, there is no significant difference among the classification results by four combinations.

IV. DISCUSSION

A. Comparison of the Results by the Single-Parameter and Multiple-Parameter Methods

Based on Figs. 4 and 6 and Tables III and IV, we determined that most of the classification results (MLs # 2, 3, and 5–7) by the single-parameter method are similar to those obtained by the multiple-parameter method, which suggests no significant difference between the two methods. Further work is needed due to the limited nature of the experiment.

However, for MLs #1 and 4, the multiple-parameter method could improve the classification accuracy and reduce the ratio of the periods that are classified incorrectly, compared with the single-parameter method. From Table I, ML #4 has the shortest length (0.59 km) among the seven links and the frequency of ML #1 is 15 GHz, which is the lowest frequency with a relatively short link length. We may conclude that the multiple-parameter method could improve the classification accuracy for the link with the short length and low frequency. However, further research should be conducted.

B. Influence of Link Frequency and Length

The link with the shorter length and lower frequency has a smaller attenuation, in the same weather condition, which could influence the classification results [7], [37]. As given in Table I, there are two links at 15 GHz, one link at 18 GHz, and four links at 23 GHz, which may imply that the links at high frequency

are more suitable for monitoring the rainfall. The conclusion is similar to that obtained in [37] that the root-mean-square errors of the rainfall estimation by ML are smaller with an increase in the frequency of the ML below 30 GHz. The higher the frequency is, the stronger the attenuation effect of the rain particles is, which increases the total attenuation of the link, and simplifies to the classification of the wet and dry periods by the attenuation. In addition, the classification results of the short links are less suitable to those of the long links, as shown in Figs. 5 and 6. Similar to the frequency, the longer the link is, the higher the rain-induced attenuation is, which increases the total attenuation of the link. Based on the analysis, the link with the higher frequency and the longer length is more suitable for the classification of wet and dry periods.

C. Comparisons With Other Methods

Many studies about wet/dry classification by MLs have been conducted. Cherkassky *et al.* [18] focused on the challenge of the precipitation classification using MLs and proposed a classification method based on the kernel Fisher discriminant analysis based on the network of MLs. The classification method can not only detect the wet and dry periods but also classify the rain, snow, and sleet with a good agreement (85%). The method employed in our study is a special case of [18]. In our study, we use the single-link to classify the wet and dry periods with a classification agreement, which is higher than 90%. In [38], a method to classify dry and rainy periods has been presented. The method can be applied in real time by the single ML and does not require any additional data for the calibration. The method can detect about 92% of all rainy periods. It is an efficient technique for estimating the baseline. The standard deviation of the attenuation has been used for the classification in [38], which, however, contradicts the conclusion because the raindrop size distribution of the rainfall in China may be different from that in Europe. The MLs in our study are installed in urban areas and the electromagnetic environment is complex, which may cause small changes compared with the MLs in [38]. The power measurement in [38] is rounded to 1 dB and the power measurement in this study is rounded to 0.1 dB, which means that the MLs of this study may be more sensitive to the change in the electromagnetic environment. However, further work is needed due to the limited data measured by MLs.

In addition, the classification method based on the SVM is compared with the random forest classification method by using the same data. The random forest classification method is an ensemble learning method for the classification by constructing a combination of decision trees, such that each tree depends on the values of a random vector that is sampled independently with the same distribution for all trees [39]. Table V gives the classification results of Combination 4 by two methods. The results show that the values of the TPR by the SVM are higher than those by the random forest classification method, while the values of the FPR of the SVM are lower than those obtained by the random forest method, which indicates that the method based on the SVM has a higher accuracy than the random forest method for the wet/dry classification

TABLE V
CLASSIFICATION RESULTS OF COMBINATION 4 BY SVM AND RANDOM FOREST

	ML	1	2	3	4	5	6	7
TPR	SVM	0.97	0.89	0.93	0.94	0.91	0.71	0.95
	RF	0.61	0.60	0.68	0.69	0.60	0.50	0.63
FPR	SVM	0.28	0.24	0.11	0.19	0.16	0.11	0.17
	RF	0.34	0.30	0.31	0.28	0.25	0.25	0.30

RF represents random forest in the table.

V. CONCLUSION

This article proposed a method for classifying wet/dry periods by using the statistical parameters from attenuation measurements measured by MLs. First, we analyze the relation between the statistical parameters of the attenuation data from seven MLs and the wet/dry periods and determined that the mean, minimum, and maximum values of the attenuation highly relate to wet/dry periods. Second, our method adopts the SVM for the classification and applies three statistical parameters for the alternative feature vector for the SVM. Seven MLs and rain gauges are selected to test the classification method.

The results show that the accuracy of the method is higher than 0.8, which indicates a satisfactory classification result. The values of the TPR are larger than 0.7 and most of them are greater than 0.9, which indicates that the method can correctly classify wet periods. In addition, the values of the FPR are less than 0.3 and most of the values are less than 0.2, which shows that the method incorrectly classifies the dry period as the wet period with a low probability. The results elaborate that the classification method based on the statistical parameters can classify wet and dry periods with high accuracy by the single-parameter and multiple-parameter methods, which can help improve the precision of the baseline of MLs and rainfall estimation. Furthermore, we discuss the influences of the link length and frequency. We discovered that ML with a higher frequency and longer length may improve the accuracy of the classification method. Based on the study, the method can classify the wet and dry periods, and estimate a dynamic baseline attenuation with a high accuracy when the baseline is needed for retrieving the path-averaged rain rate. Meanwhile, because the method has been trained before the classification, we can select the optimal combination of the statistical parameters of the attenuation data compared with the other methods. The study preliminarily proves the feasibility of using MLs to detect rain, although additional work is needed. Because this study is carried out in China, the applicability of MLs in the rainfall estimation in less traditional places is promoted from the ML-community perspective.

ACKNOWLEDGMENT

The authors would like to thank anonymous reviewers for providing helpful advice.

REFERENCES

- [1] O. Goldshtein, H. Messer, and A. Zinevich, "Rain rate estimation using measurements from commercial telecommunications links," *IEEE Trans. Signal Process.*, vol. 57, no. 4, pp. 1616–1625, Apr. 2009.

- [2] C. Lorenz and H. Kunstmann, "The hydrological cycle in three state-of-the-art reanalyses: Intercomparison and performance analysis," *J. Hydrometeorol.*, vol. 13, no. 5, pp. 1397–1420, Oct. 2012, doi: [10.1175/JHM-D-11-088.1](https://doi.org/10.1175/JHM-D-11-088.1).
- [3] E. N. Anagnostou, W. F. Krajewski, and J. Smith, "Uncertainty quantification of mean-areal radar-rainfall estimates," *J. Atmos. Ocean. Technol.*, vol. 16, pp. 206–215, 1999.
- [4] E. Anagnostou and W. Krajewski, "Real-time radar rainfall estimation. Part II: Case study," *J. Atmos. Ocean. Technol.*, vol. 16, pp. 198–205, 1999.
- [5] A. Y. Hou *et al.*, "The global precipitation measurement mission," *Bull. Amer. Meteorol. Soc.*, vol. 95, no. 5, pp. 701–722, May 2014, doi: [10.1175/BAMS-D-13-00164.1](https://doi.org/10.1175/BAMS-D-13-00164.1).
- [6] H. Messer, A. Zinevich, and P. Alpert, "Environmental monitoring by wireless communication networks," *Science*, vol. 312, p. 713, 2006.
- [7] A. Berne and R. Uijlenhoet, "Path-averaged rainfall estimation using microwave links: Uncertainty due to spatial rainfall variability," *Geophys. Res. Lett.*, vol. 34, no. 7, 2007, Art. no. L07403.
- [8] H. Leijnse, R. Uijlenhoet, and J. N. M. Stricker, "Hydrometeorological application of a microwave link: 2. Precipitation," *Water Resour. Res.*, vol. 43, no. 4, pp. 244–247, 2007.
- [9] R. Uijlenhoet, A. Overeem, and H. Leijnse, "Opportunistic remote sensing of rainfall using microwave links from cellular communication networks," *WIREs Water*, vol. 5, 2018, Art. no. e1289, doi: <https://doi.org/10.1002/wat2.1289>.
- [10] H. Messer, "Rainfall monitoring using cellular networks," *IEEE Signal Process. Mag.*, vol. 24, no. 3, pp. 142–144, May 2007.
- [11] A. Zinevich, H. Messer, and P. Alpert, "Frontal rainfall observation by a commercial microwave communication network," *J. Appl. Meteorol. Climatol.*, vol. 48, pp. 1317–1334, 2009.
- [12] A. Overeem, H. Leijnse, and R. Uijlenhoet, "Retrieval algorithm for rainfall mapping from microwave links in a cellular communication network," *Atmos. Meas. Techn.*, vol. 9, no. 5, pp. 2425–2444, 2016, doi: [10.5194/amt-9-2425-2016](https://doi.org/10.5194/amt-9-2425-2016).
- [13] A. Overeem, H. Leijnse, and R. Uijlenhoet, "Two and a half years of country-wide rainfall maps using radio links from commercial cellular telecommunication networks," *Water Resour. Res.*, vol. 52, pp. 8039–8065, 2016.
- [14] M. F. R. Gaona, A. Overeem, T. H. Raupach, H. Leijnse, and R. Uijlenhoet, "Rainfall retrieval with commercial microwave links in São Paulo, Brazil," *Atmos. Meas. Techn.*, vol. 11, pp. 4465–4476, 2018, doi: <https://doi.org/10.5194/amt-11-4465-2018>.
- [15] K. Song, X. Liu, T. Gao, and B. He, "Rainfall estimation using a microwave link based on an improved rain-induced attenuation model," *Remote Sens. Lett.*, vol. 10, no. 11, pp. 1057–1066, 2019, doi: [10.1080/2150704X.2019.1648902](https://doi.org/10.1080/2150704X.2019.1648902).
- [16] L. Barthès and C. Mallet, "Rainfall measurement from the opportunistic use of an Earth-space link in the Ku band," *Atmos. Meas. Techn.*, vol. 6, pp. 2181–2193, 2013.
- [17] Y. Liberman, R. Samuels, P. Alpert, and H. Messer, "New algorithm for integration between wireless microwave sensor network and radar for improved rainfall measurement and mapping," *Atmos. Meas. Techn.*, vol. 7, pp. 3549–3563, 2014.
- [18] D. Cherkassky, J. Ostrometzky, and H. Messer, "Precipitation classification using measurements from commercial microwave links," *IEEE Trans. Geosci. Remote Sens.*, vol. 52, no. 5, pp. 2350–2356, May 2014.
- [19] T. C. van Leth, A. Overeem, H. Leijnse, and R. Uijlenhoet, "A measurement campaign to assess sources of error in microwave link rainfall estimation," *Atmos. Meas. Techn.*, vol. 11, no. 8, pp. 4645–4669, Aug. 2018, doi: [10.5194/amt-11-4645-2018](https://doi.org/10.5194/amt-11-4645-2018).
- [20] C. Chwala *et al.*, "Precipitation observation using microwave backhaul links in the alpine and pre-alpine region of southern Germany," *Hydrol. Earth Syst. Sci.*, vol. 16, pp. 2647–2661, 2012.
- [21] Z. Wang, M. Schleiss, J. Jaffrain, A. Berne, and J. Rieckermann, "Using Markov switching models to infer dry and rainy periods from telecommunication microwave link signals," *Atmos. Meas. Techn.*, vol. 5, pp. 1847–1859, 2012.
- [22] O. Harel and H. Messer, "Extension of the MFLRT to detect an unknown deterministic signal using multiple sensors, applied for precipitation detection," *IEEE Signal Process. Lett.*, vol. 20, no. 10, pp. 945–948, Oct. 2013.
- [23] J. Ostrometzky, D. Cherkassky, and H. Messer, "Accumulated mixed precipitation estimation using measurements from multiple microwave links," *Adv. Meteorol.*, vol. 2015, 2015, Art. no. 707646.
- [24] B. Choubin, E. Moradi, M. Golshan, J. Adamowski, F. Sajedi-Hosseini, and A. Mosavi, "An ensemble prediction of flood susceptibility using multivariate discriminant analysis, classification and regression trees, and support vector machines," *Sci. Total Environ.*, vol. 651, pp. 2087–2096, Feb. 2019, doi: [10.1016/j.scitotenv.2018.10.064](https://doi.org/10.1016/j.scitotenv.2018.10.064).
- [25] K. Song, T.-C. Gao, X. Liu, M. Yin, and Y. Xue, "Method and experiment of rainfall inversion using a microwave link based on support vector machine," *Acta Physica Sinica*, vol. 64, no. 24, 2015, Art. no. 244301.
- [26] H. Leijnse, R. Uijlenhoet, and J. N. M. Stricker, "Microwave link rainfall estimation: Effects of link length and frequency, temporal sampling, power resolution, and wet antenna attenuation," *Adv. Water Resour.*, vol. 31, pp. 1481–1493, 2008.
- [27] C. Chwala and H. Kunstmann, "Commercial microwave link networks for rainfall observation: Assessment of the current status and future challenges," *WIREs Water*, vol. 6, 2019, Art. no. e1337.
- [28] M. Fencel, M. Dohnal, P. Valtr, M. Grabner, and V. Bares, "Atmospheric observations with E-band microwave links—challenges and opportunities," *Atmos. Meas. Techn. Discuss.*, vol. 2020, pp. 1–29, 2020, doi: doi.org/10.5194/amt-2020-28.
- [29] H. Leijnse, R. Uijlenhoet, and J. N. M. Stricker, "Rainfall measurement using radio links from cellular communication networks," *Water Resour. Res.*, vol. 43, no. 3, 2007, Art. no. W03201.
- [30] J. A. Rice, *Mathematical Statistics and Data Analysis*, 3rd ed. Boston, MA, USA: Cengage Learning, 2006.
- [31] X. R. Zhao, Z. Sheng, J. W. Li, H. Yu, and K. J. Wei, "Determination of the "wave turbopause" using a numerical differentiation method," *J. Geophys. Res., Atmos.*, vol. 124, pp. 10592–10607, 2019.
- [32] V. N. Vapnik, *The Nature of Statistical Learning Theory*. New York, NY, USA: Springer, 2013.
- [33] T. Kavzoglu, E. K. Sahin, and I. Colkesen, "Landslide susceptibility mapping using GIS-based multi-criteria decision analysis, support vector machines, and logistic regression," *Landslides*, vol. 11, no. 3, pp. 425–439, 2014.
- [34] K. Song, X. Liu, T. Gao, M. Yin, and B. He, "The feasibility analysis of cellphone signal to detect the rain: Experimental study," *IEEE Geosci. Remote Sens. Lett.*, vol. 17, no. 7, pp. 1158–1162, Jul. 2020.
- [35] J. Ostrometzky and H. Messer, "Dynamic determination of the baseline level in microwave links for rain monitoring from minimum attenuation values," *IEEE J. Sel. Topics Appl. Earth Observ. Remote Sens.*, vol. 11, no. 1, pp. 24–33, Jan. 2018.
- [36] J. Ostrometzky and H. Messer, "On the information in extreme measurements for parameter estimation," *J. Franklin Inst.*, vol. 357, no. 1, pp. 748–771, 2020.
- [37] H. Leijnse, R. Uijlenhoet, and A. Berne, "Errors and uncertainties in microwave link rainfall estimation explored using drop size measurements and high-resolution radar data," *J. Hydrometeorol.*, vol. 11, no. 6, pp. 1330–1344, 2010.
- [38] M. Schleiss and A. Berne, "Identification of dry and rainy periods using telecommunication microwave links," *IEEE Geosci. Remote Sens. Lett.*, vol. 7, no. 3, pp. 611–615, Jul. 2010.
- [39] L. Breiman, "Random forests," *Mach. Learn.*, vol. 45, no. 1, pp. 5–32, 2001.



Kun Song received the B.S. and M. S. degrees in atmospheric measurement techniques from the PLA University of Science and Technology, Nanjing, China, in 2014 and 2017, respectively. He is currently working toward the Ph.D. degree in atmosphere science with the National University of Defense Technology, Changsha, China.

His research interests include atmospheric science, atmospheric measurement, and remote sensing techniques and instruments.



Xichuan Liu received the master's and Ph.D. degrees in atmospheric measurement techniques from the PLA University of Science and Technology, Nanjing, China, in 2010 and 2014, respectively.

He is currently a Lecturer with the College of Meteorology and Oceanography, National University of Defense Technology, Nanjing, China. His research interests include atmospheric physics, atmospheric measurement, and remote sensing techniques and instruments.



Haonan Wu was born in 1993. She received the B.A. degree in Chinese language and literature from the Suzhou University of Science and Technology, Suzhou, China, in 2016.

She is currently working with Weizhirun Intelligent Technology Company, Ltd., Jiangyin, China.



Mingzhong Zou received M.S. degree in agricultural information from China Agricultural University, Beijing, China, in 2009. He is a Senior Engineer with Water Resources Bureau, Jiangyin, China.

Ding Zhou received the B.S. degree in computer science and technology from Jiangsu University of Science and Technology, Zhenjiang, China, in 2008.

He is currently working with Weizhirun Intelligent Technology Company, Ltd., Jiangyin, China. He is focusing on intelligent water conservancy and intelligent agriculture system solutions.



Feng Ji was born in 1972. He received the Associate degree in computer science and technology from the College of Meteorology, Nanjing, China, in 1995.

He is currently working with Weizhirun Intelligent Technology Company, Ltd., Jiangyin, China.